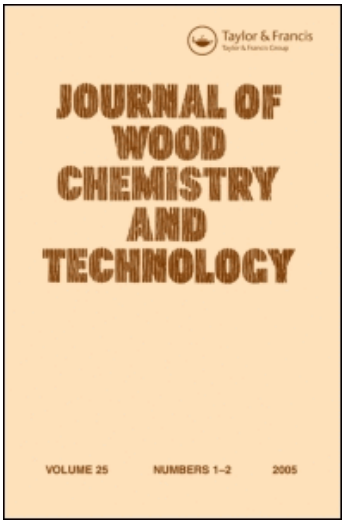

Journal of Wood Chemistry and Technology
Publication details, including instructions for authors and subscription information:
http://www.informaworld.com/smpp/title~content=t713597282

Polyoxometalate (POM) Oxidation of Phenols: Effect of Aromatic Substituent Groups on Reaction Mechanism

Yong Sik Kim[a]; Hou-min Chang[b]; John F. Kadla[a]
[a] Faculty of Forestry, University of British Columbia, Vancouver, BC, Canada [b] College of Natural Resources, North Carolina State University, Raleigh, North Carolina, USA

To cite this Article Kim, Yong Sik , Chang, Hou-min and Kadla, John F.(2008) 'Polyoxometalate (POM) Oxidation of Phenols: Effect of Aromatic Substituent Groups on Reaction Mechanism', Journal of Wood Chemistry and Technology, 28: 1, 1 — 25
To link to this Article: DOI: 10.1080/02773810801916332
URL: http://dx.doi.org/10.1080/02773810801916332

Journal of Wood Chemistry and Technology, 28: 1–25, 2008

ISSN 0277-3813 print/1532-2319 online
DOI: 10.1080/02773810801916332

Polyoxometalate (POM) Oxidation of Phenols: Effect of Aromatic Substituent Groups on Reaction Mechanism

Yong Sik Kim,[1] Hou-min Chang,[2] and John F. Kadla[1]

[1]Faculty of Forestry, University of British Columbia, Vancouver, BC, Canada
[2]College of Natural Resources, North Carolina State University, Raleigh, North Carolina, USA

Abstract: The kinetics of the oxidation of a series of substituted phenols by polyoxometalate (POM), $K_5[SiVW_{11}O_{40}] \cdot 12H_2O$ were investigated. Under all conditions studied second-order kinetics were observed. Electron-transfer from neutral phenols (k_1) was slower than that from the corresponding phenoxide anions (k_2), and the reaction rate was highly dependent on the nature of the substituent groups. The observed rate constants decreased in the order: *p*-methoxyphenol (***1***) > *p*-methylphenol (***2***) > *m*-methylphenol (***4***) > *m*-methoxyphenol (***3***) > phenol (***5***) > *p*-chlorophenol (***6***) > *p*-bromophenol (***7***) > *m*-chlorophenol (***8***) > *m*-nitrophenol (***9***). A *Hammett* plot of the data revealed a better correlation with σ^+ than with σ, suggesting a reaction involving the formation of an electron-deficient radical intermediate with the rate-determining step being an electron-transfer from a neutral substrate. Depending on the concentration of POM, oxidized phenolic and oxidative coupling products were detected.

Keywords: Kinetics, mechanism, oxidation, polyoxometalate (POM), substituted phenols

We gratefully acknowledge Professor Brian James for his input and discussion of the kinetic analysis, and NSERC for support.

Address correspondence to John F. Kadla, Faculty of Forestry, University of British Columbia, Vancouver, BC, Canada. E-mail: john.kadla@ubc.ca

INTRODUCTION

Polyoxometalates (POMs) are a rapidly growing class of metal-oxygen-cluster anions.[1–4] They are synthetic inorganic compounds that contain highly symmetrical core assemblies of MO(x) units (M = Vanadium, Molybdenum, Tungsten) and react as outer-sphere electron-transfer oxidants and catalysts.[4–7] The properties of POMs can be controlled by altering the POM composition and structure.[5,8] As a result, polyoxometalates have found applications in analytical and clinical chemistry, catalysis (including photocatalysis), biochemistry (electron transport inhibition), medicine (anti-tumor, anti-viral, and even anti-HIV activity), and solid-state devices.[9]

Over the last decade there has been an increasing interest in the application of POMs in the catalytic delignification of wood pulp.[10–12] POMs offer a safe and environmentally benign alternative to traditional bleaching reagents such as elemental chlorine. Efficient and selective removal of lignin, an aromatic polyol, from wood pulps without severe degradation to carbohydrates (e.g., cellulose) can be accomplished using POMs under anaerobic and aerobic conditions.[10–12] The catalytic mechanism involves a series of redox cycles wherein the reduction of the $POM_{(ox)}$ by the substrate (lignin) is accompanied by subsequent reoxidation of the $POM_{(red)}$ by O_2 – the total electron transfer if from substrate to O_2.

Several investigations into the mechanisms of POM oxidations of phenolic compounds have been reported.[13–18] Reportedly, POM oxidation of phenolic compounds proceeds via either hydrogen atom transfer or proton coupled electron transfer mechanisms. The oxidized resonance stabilized phenoxy radical intermediate then undergoes (i) a second oxidation step to the corresponding cation and subsequent benzoquinone formation, or (ii) radical coupling with a second oxidized phenol and dimer[13–15]/oligomer[15] formation. The resulting dimeric/oligomeric compounds can be subsequently oxidized, and undergo the same oxidative reaction steps as the initial phenol. Although a number of studies on the reactions of POMs with phenolic lignin model compounds have been reported,[13–18] very little information is available on the effect of phenolic compound structure on reaction mechanism and kinetics. As lignin is a cross linked highly functionalized macromolecule containing methoxyl, hydroxyl, carbonyl, and various functionalized aliphatic side-chains,[19–22] a comprehensive understanding of substrate structure on the reaction/oxidation kinetics is critical to further develop this technology.

In this article, we report the results of a study on the kinetics and mechanism of the oxidation of substituted phenols in aqueous solutions by POM ($K_5[SiVW_{11}O_{40}] \cdot 12H_2O$). Of particular interest is the relationship between phenol substitutent groups and reaction kinetics. Using the *Hammett* equation, the relationship between electron density of substituted phenols and POM oxidation rate is reported.

EXPERIMENTAL

Materials

$K_5[SiVW_{11}O_{40}] \cdot 12H_2O$ (POM) was provided from the USDA Forest Products Laboratory (Madison WI, US).[10] The aromatic compounds: *p*-methoxyphenol (***1***), *p*-methylphenol (***2***), *m*-methoxyphenol (***3***), *m*-methylphenol (***4***), phenol (***5***), *p*-chlorophenol (***6***), *p*-bromophneol (***7***), *m*-chlorophenol (***8***), *p*-nitrophenol (***9***), and 1,4-benzoquinone (***10***) were purchased from Aldrich Chemicals. $CDCl_3$, DMSO-d_6, and acetone-d_6 were purchased from Cambridge Isotope Laboratories. All other chemicals were purchased from either Fisher Scientific or Sigma-Aldrich and used as received.

Sodium Acetate-Acetic Acid Buffer System

All the kinetic reactions were carried out in a sodium acetate-acetic acid buffer system. The pH range used was 3.8–6.0, and adjusted by adding acetic acid to a 0.2 M sodium acetate stock solution. pH values were measured using a Fisher pH meter, model Accumet AR 15.

Kinetic Measurements

Kinetic reactions were carried out using a dual-syringe stopped-flow apparatus equipped with a mixing chamber and attached to a 2 cm^3 cuvette (quartz micro flow cell). The temperature was maintained over a range of 4–90 $\pm$ 1°C by a Haake D1/G recirculating refrigerated bath. Absorbance measurements were performed on a PerkinElmer Lambda 45 UV/VIS spectrophotometer with a cell pathlength of 1 cm. In a typical kinetic experiment (pseudo-first order conditions), equal volumes (3 mL) of the phenolic substrate (73.5 μmol) in acetate buffer (0.2 M, pH 5) and POM (1.5 μmol) acetate buffer solution (0.2 M, pH 5) were mixed using the dual-syringe stopped-flow apparatus. Prior to mixing all phenolic and POM buffer solutions were thoroughly purged with argon and equilibrated for at least 2 h at the reaction temperature in a MaxQ™ 4000 Incubated and Refrigerated Shaker (Barnstead/Lab-Line co.). For slow reacting model compounds (e.g., ***8*** and ***9***), a 1.9 mL aliquot of degassed phenolic compound (24.5 μmol) was loaded into a 5 mL quartz cuvette and sealed with a rubber septum. The cuvette was put into the UV and equilibrated at the reaction temperature for at least 2 h. Reactions were initiated by injecting 0.1 mL of a POM (0.5 μmol) stock solution and manually mixed. The final concentrations of the phenolic compounds and POM were 12.25 mmol L^{-1} and 0.25 mmol L^{-1}, respectively (49 molar equivalents of phenolic substrate to POM).

Reaction kinetics were spectrophotometrically recorded by monitoring the decrease in absorbance of the oxidized POM at 350 nm or the increase in

absorbance of the reduced POM at 520 nm. Data were recorded every 0.1–600 s for 0.5 to 50 h, depending on the experiment. Reactions involving compounds ***1***–***9*** were run in acetate buffered solution (0.2 M, pH 5.0). All reactions were run in triplicate and rate constants reported as average values. Prior to kinetic analysis the extinction coefficient (ε) for the oxidized POM ($\varepsilon = 2630\ M^{-1}\ cm^{-1}$ at 350 nm) and reduced POM ($\varepsilon = 610\ M^{-1}\ cm^{-1}$ at 520 nm) was determined from linear regression of the plots of absorbance versus concentration of POM (see Appendix).

Reaction Order

The reaction order with respect to phenol (***5***) and POM were determined by the plotting initial rate versus concentration of POM or phenol according to the initial rate law (see appendix). First, the POM concentration was held constant at 0.25 mmol L^{-1}, while the concentration of the phenolic compound was varied, for example, [***5***] was varied from 9.0 to 45 mmol L^{-1}. Then, the phenolic concentration was held constant at 15 mmol L^{-1} and the concentration of the POM varied from 1.25 to 6.25 mmol L^{-1}.

Reaction Rate

Reaction rates were measured using pseudo-first order and second-order reaction conditions. Rate constants (k_{obs}) were determined by fitting a straight line through the initial 25–50% POM conversion (see Appendix). Under pseudo-first order conditions $\ln[(POM_o)/(POM)]$ versus time plots were used, while second-order rate constants (k) were calculated from either $k = (\text{initial rate})/(2 \cdot [POM] \cdot [\text{phenol}])$ or $k = k_{obs}/(2 \cdot [\text{phenol}])$.

Effect of pH

As outlined in Scheme 1 the oxidation of phenols is dependent on pH (5, 15, 16). To evaluate the effect of pH on the reaction rates, POM oxidation of compounds ***1***, ***2***, ***5***, and ***8*** were studied over the pH range 3.8–6.0 at 20, 35, 45, and 80°C. The pH of the acetate buffer (0.2 M) was adjusted by adding acetic acid. The concentrations of the phenolic compounds and POM were 12.25 mmol L^{-1} and 0.25 mmol L^{-1}, respectively (49 molar equivalents of phenolic substrate to POM).

Kinetic Model

According to Scheme 1 two equivalents of POM are required to fully oxidize phenols. The overall reaction can be represented by Eq. (1).[5,15]

$$x\text{-}C_6H_4\text{-}OH + 2(SiVW_{11}O_{40}^{5-}) \xrightarrow{k} \text{products} + 2(SiVW_{11}O_{40}^{6-}) + H^+ \quad (1)$$

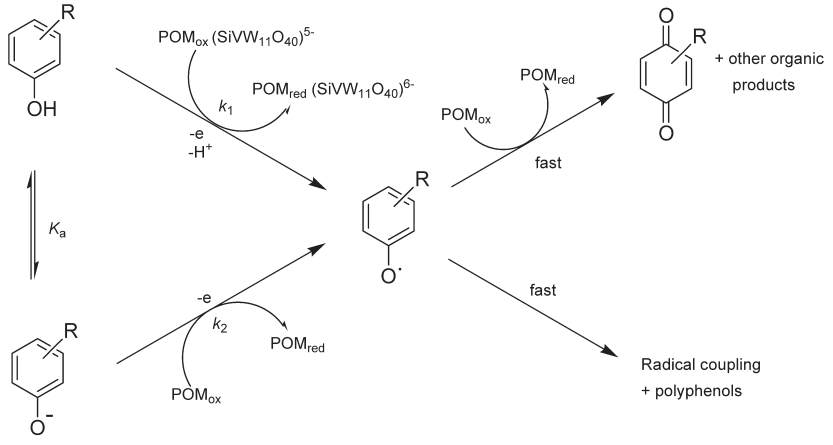

R = H, OCH_3, CH_3, Cl, Br, NO_2

Scheme 1. Possible reaction mechanism for POM ($SiVW_{11}O_{40}^{5-}$) oxidation of phenols.

Accordingly, Eq. (1) can be written as the rate law Eq. (2).

$$\frac{d[SiVW_{11}O_{40}^{6-}]}{dt} = 2\,k[SiVW_{11}O_{40}^{5-}]^a[x\text{-}C_6H_4\text{-}OH]^b \tag{2}$$

The reaction order (a and b) of each reactant can be calculated from the initial rate Eq. (3)

$$\begin{aligned} &v = k'[SiVW_{11}O_{40}^{5-}]^a,\ k' = 2\,k[x\text{-}C_6H_4\text{-}OH]_o^b \quad \text{or} \\ &v = k''[x\text{-}C_6H_4\text{-}OH]^b\, k''\,[SiVW_{11}O_{40}^{5-}]_o^a \end{aligned} \tag{3}$$

The second-order rate expression (a = b = 1) can be expressed as Eq. (4).

$$\frac{d[SiVW_{11}O_{40}^{6-}]}{dt} = 2\,k[SiVW_{11}O_{40}^{5-}][x\text{-}C_6H_4\text{-}OH] \tag{4}$$

Under pseudo-first order conditions, that is, >10-fold excess of phenolic substrate Eq. (4) can be written as Eq. (5).

$$\begin{aligned} &\frac{d[SiVW_{11}O_{40}^{6-}]}{dt} = k_{obs}[SiVW_{11}O_{40}^{5-}] \quad \text{or} \\ &\ln\frac{[SiVW_{11}O_{40}^{5}]}{[SiVW_{11}O_{40}^{5}]_o} = k_{obs}t \end{aligned} \tag{5}$$

Further, based on the relationship between Eqs. (4) and (5), the observed pseudo-first order rate constant (k_{obs}) can be expressed according to Eq. (6).

$$k_{obs} = 2k[x\text{-}C_6H_4\text{-}OH] \tag{6}$$

Calculation of k_1 and k_2

The oxidation of phenols can occur through reaction with either the neutral phenol or phenolate ion. Using a steady-state approximation for the initial oxidized intermediates, that is, $-d[x\text{-}C_6H_4\text{-}OH^+]/dt = -d[x\text{-}C_6H_4\text{-}O^\cdot]/dt = 0$, the following expression can be obtained.[23,24]

$$\frac{d[SiVW_{11}O_{40}^{6-}]}{dt} = 2\left(k_1 + \frac{k_2K_a}{[H^+]}\right)[SiVW_{11}O_{40}^{5-}][x\text{-}C_6H_4\text{-}OH] \quad (7)$$

where K_a is the acid dissociation constant of the phenol and k_1 and k_2 are the rate constants for the oxidation of $x\text{-}C_6H_4\text{-}OH$ and $x\text{-}C_6H_4\text{-}O^-$, respectively (Scheme 1). The rate of POM reduction (phenol oxidation) is dependent on the pH of the reaction system, therefore the observed second-order rate constant can be expressed as Eq. (8).

$$k = \left(k_1 + \frac{k_2K_a}{[H^+]}\right) \quad (8)$$

Product Analysis

Depending on the reactivity of the phenol, different reaction conditions were used to ensure sufficient oxidation/product formation. In a typical reaction, the substituted phenol (0.4 mmol) was dissolved in 1 mL of ethanol (to ensure dissolution) and added via syringe to a sealed reaction flask containing POM (1.6 mmol) dissolved in acetate buffered solution (80 mL, pH 5.0, 0.2 M). All air was displaced by purging with argon. The final concentration of the phenol and POM were ~5.0 mmol L^{-1} and ~20 mmol L^{-1}, respectively. For compound ***1*** the reaction mixture was agitated for 1 h at room temperature, while compounds ***4*** and ***5*** were reacted for 2 and 5 h at 60°C, respectively. At the end of the reaction, the solutions were filtered using a nylon membrane filter (0.45 μm, 47 mm), and any precipitated products were washed repeatedly with deionized water, isolated and freeze-dried using a VirTis EX freeze-dryer. The filtrate (~80 ml) was acidified to pH 2 with concentrated HCl and diluted with a 2:1 (v/v) mixture of chloroform and acetone (70 mL). The organic phase was separated, and the aqueous layer was repeatedly extracted with a 2:1 (v/v) mixture of chloroform and acetone (2 × 70 mL). The organic phases were combined, dried over anhydrous $MgSO_4$, filtered and concentrated under reduced pressure to approximately 3 mL; the crude product mixture. A portion of the crude product mixture was then analyzed by GC-MS; one sample (~1 mL) was analyzed directly, while a second sample (~1 mL) was first silylated by reacting with N,O-bis(trimethylsilyl)acetamide (200 μL) in pyridine (0.5 mL) at room temperature for 24 h. The remaining reaction product mixture (~1 mL) was separated, if possible, by thin layer chromatography (eluent: 5% acetone in $CHCl_3$) and analyzed by NMR.

Analytical Methods

Gas chromatography-mass spectroscopy (GC-MS) analyses were conducted using a ThermoFinnigan TraceGC and PolarisQ ion-trap mass spectrometer. GC analyses were performed with a J&W Scientific Inc. DB-5 column (30 m × 0.32 mm × 0.25 μm). The injection temperature was set to 200°C, the transfer line temperature to 200°C, and the ion source to 300°C. The Helium flow was 1 mL min^{-1}. After a 5 min solvent delay at 70°C, the oven temperature was increased at 5°C min^{-1} to 280°C and held at temperature for 5 min prior to being cooled down to 70°C. Mass spectra were recorded from $m/z = 50$ to 650 at 0.58 s $scan^{-1}$ with an electron ionization of 70 eV. When available, commercial samples of identified products were used to verify chromatographic retention time and spectral data.

^{1}H and ^{13}C nuclear magnetic resonance (NMR) analyses of isolated products were conducted on a Bruker AVANCE 300 MHz spectrometer at 300 K using $CDCl_3$, acetone-d_6 or DMSO-d_6 as the solvent. Chemical shifts were referenced to tetramethylsilane (TMS; 0.0 ppm).

The average molecular mass and distribution of the products were determined by gel permeation chromatography (GPC; Agilent 1100, UV and RI detectors). Chromatographic separation was performed using styragel columns (Styragel HR 4 and HR 2) at 35°C, THF (HPLC Grade) as the eluting solvent (0.5 mL min^{-1}) and UV detection at 280 nm. Sample concentration was 1 mg mL^{-1} and the injection volume was 75 μL. The GPC system was calibrated using standard polystyrene samples (Showa Denko) with molecular weights ranging between 580 and 1,800,000 Daltons.

MALDI-TOF (matrix-assisted laser desorption ionization time-of-flight) mass spectrometry analyses were obtained on an Applied Biosystems Voyager System 4311 with linear geometry (positive polarity). Matrices were prepared using 2 mg samples dissolved in 10 mL of THF. A 1 μL sample solution was mixed with 3,5-dimethoxy-4-hydroxycinnamic acid (sinapic acid) and/or 2,5-dihydroxybenzoic acid (gentistic acid) matrix, in a matrix-to-analyte ratio of 1:1. One μL of the mixture was spotted on a stainless steel plate and inserted into the instrument.

Identification of Reaction Products

1,4-Benzoquinone (***10***)

EI-MS m/z (low resolution) 108(M^+, 75), 80(76), 52(100). Compound identification was confirmed using a commercial sample (Aldrich) and comparing the chromatographic retention time and spectral data.

2-(2-Hydroxy-5-methoxy-phenyl)-[1,4]benzoquinone (***11***)

EI-MS m/z (low resolution) 230 (M^+, 100), 215 (10), 202 (30), 187 (45), 174 (9), 159 (14), 148 (10), 131 (8), 107(6), 95 (5), 79 (11), 63 (5), 51 (9); ^{1}H-NMR: (DMSO) δ 3.78(3H, s, OCH_3), 5.48 (1H, d, OH), 6.78 (1H, dd, J = 3.0 Hz, 10.2 Hz, ArH), 6.91(1H, d, J = 10.2 Hz, ArH), 7.03 (4H, m, ArH)); ^{13}C-NMR: (DMSO) δ 55.67, 110.79 115.32, 121.81, 134.53, 137.07, 145.65, 157.86, 159.09, 181.76, 187.61.

5,5′-Dimethoxy-biphenyl-2,2′-diol (***12***)

EI-MS m/z (low resolution) 246 (M^+, 100), 108 (40), 78 (7); ^{1}H-NMR: ($CDCl_3$) δ 3.81(6H, s, OCH_3), 5.24 (2H, d, OH), 6.84 (6H, m, ArH); ^{13}C-NMR: ($CDCl_3$) δ 55.97, 115.57, 115.91, 117.80, 124.62, 146.56, 154.19. The assignments are in agreement with literature data.[25]

Biphenyl-2,2′-diol (***13***)

EI-MS m/z (low resolution) trimethyl silyl ether: 330 (M^+, 71), 315 (42), 242 (7), 227 (19), 147 (7), 73 (100)); ^{1}H-NMR: (acetone-d_6) δ 6.95 (4H, m, ArH), 7.22 (4H, m, ArH); ^{13}C-NMR: (acetone-d_6) δ 116.86, 120.39, 126.23, 128.69, 131.65, 153.96. Compound identification was confirmed using a commercial sample (Aldrich) and comparing the chromatographic retention time and spectral data.

Dimers (***14****)

Dimers formed during the POM ($SiVW_{11}O_{40}^{5-}$) oxidation of 4 (m-methylphenol) as listed in Table A1 (see Appendix).

RESULTS AND DISCUSSION

Kinetics and Mechanism

Figure 1 shows the change in absorbance for aqueous solutions (pH 5.0) of POM (0.25 mmol L^{-1}) and ***2*** and ***5*** (12.25 mmol L^{-1}) at 25°C and 45°C, respectively. On mixing with excess phenol, there is a decrease in absorbance at 350 nm (peak of oxidized POM) with a concurrent increase in absorbance at 520 nm (reduced POM). For ***2*** an isosbestic point is observed at 446 nm, while for ***5*** it is not clearly seen. In ***5*** the point of intersection was observed at 446 nm early in the reaction and 457 nm late in the reaction (Figure 1b). A similar phenomena was observed in the reaction of phenol with a platinum (III) dinuclear complex.[26] This shift in isosbestic point was attributed to a reaction system that proceeds via at least two steps.

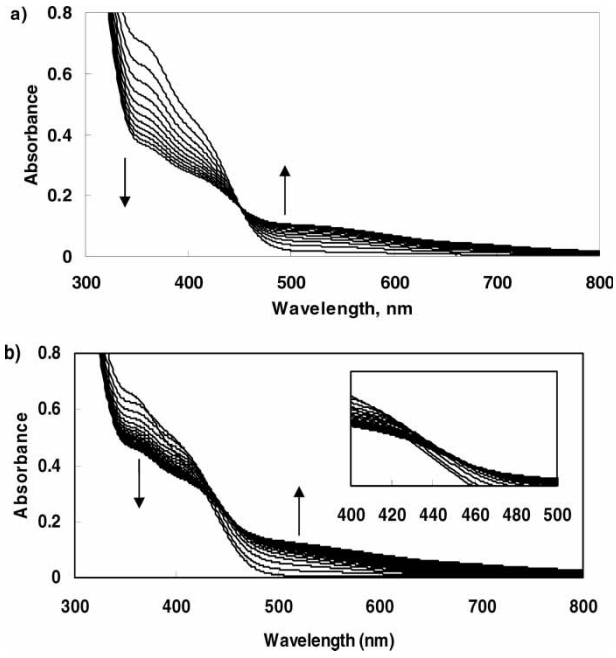

Figure 1. Change in POM ($SiVW_{11}O_{40}^{5-}$) absorbance during reaction with a) ***2*** and b) ***5*** in sodium acetate buffer (0.2 M, pH 5.0) at 25°C and 45°C, respectively. ([***2***] = [***5***] = 12.25 mmol L^{-1}, [POM] = 0.25 mmol L^{-1}). The arrows indicate the decrease (↓) in absorbance of the oxidized POM at 350 nm and the increase (↑) in absorbance of the reduced POM at 520 nm, respectively.

POM oxidation with phenols is known to proceed via an electron-transfer mechanism.[5,15,16] In aqueous conditions neutral phenols and phenoxide anions exist in a rapid-equilibrium, where the concentration of each is pH dependent.[27] Both neutral phenols and phenoxide anions can react with the POM to give a phenoxy radical intermediate. Possible reaction pathways are shown in Scheme 1.

According to Scheme 1 two equivalents of POM are required to fully oxidize phenols. The first step in evaluating the reaction kinetics of POM oxidation of the various phenols was to determine the respective reaction orders. This was accomplished by determining the initial rates of reaction between POM and the phenols using UV-VIS spectroscopy. The reaction order of each reactant was calculated from the initial rates,[28] Eq. (3). Plotting the initial rates against the concentration of phenol or POM resulted in a straight line that passed through the origin, indicative of first-order kinetics. Similarly, plots of ln[v] versus ln[POM_{ox}] or ln[substrate], respectively, also produced straight lines with slopes = 1, and indicating first-order kinetics for both POM and substrate (see Appendix).

The method of initial rates only samples a few initial data points, and might not reveal the full rate law. To avoid this, the data should be fit throughout the reaction. Another method is to force the rate law into first-order form using an excess of phenol, pseudo first-order rate law. Figure 2 shows the absorbance-time plots for the reaction of POM with ***1*** at different temperatures under pseudo-first order conditions. The pseudo-first order rate constants (k_{obs}) are determined by fitting a straight line through the initial 25–50% of $\ln[(POM_o)/(POM)]$ versus time plots (Table 1).

Table 1 lists the pseudo-first order rate constants (k_{obs}) for the reaction between POM and ***1*** in sodium acetate buffer (I = 0.2 M, pH 5.0) at various temperatures. From the pseudo-first order rate constant (k_{obs}), the second order rate constant (k) can be calculated using Eq. (6) or determined according to Eq. (4) using the initial rate method. The calculated (Eq. (7) – pseudo-first order) and measured (Eq. (3)– initial rate law) second order rate constants (k) are included in Table 1. It can be seen that values obtained by both methods are in good agreement with each other, and indicates overall second-order behavior under these conditions (Figure 3).

According to Scheme 1 the oxidation of phenols can occur through reaction with either the neutral phenol or phenolate ion. To further understand the mechanism of POM oxidation of phenols, the impact of acidity on k_1 and k_2 (Eqs. (7) and (8) for the reaction of POM with ***1***, ***2***, ***5***, and ***8*** was studied over the pH range 3.8–6.0 at 20, 35, 45, and 80°C. Figure 3 shows that the rates of oxidation of ***1***, ***2***, ***5***, and ***8*** increase linearly with decreasing $[H^+]$.

According to Eq. (8), k_1 is the y-intercept and k_2K_a is the slope of the line generated from plotting k versus $1/[H^+]$. The rate constants, k_2 were calculated using pK_a values at 25°C: 10.21, 10.14, 9.98, and 9.02 for ***1***, ***2***, ***5***, and ***8***, respectively.[29] Table 2 lists the calculated rate constants k_1 and k_2 for the POM oxidation of ***1***, ***2***, ***5***, and ***8***. It can be seen that $k_2 \gg k_1$, indicating the reaction mechanism involves a rate-determining electron transfer from neutral phenol

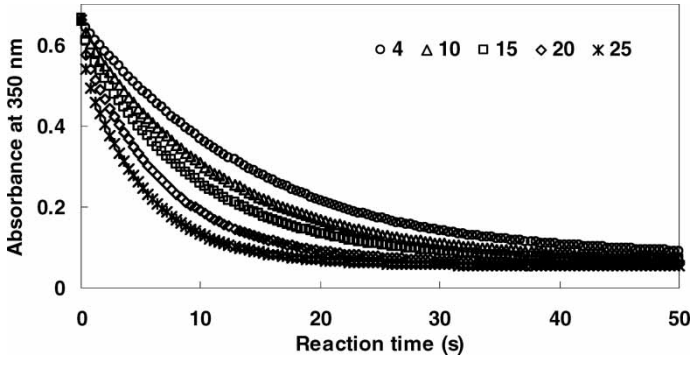

Figure 2. Absorbance-time plots for the reaction of POM ($SiVW_{11}O_{40}^{5-}$) with ***1*** at different temperatures (°C) in sodium acetate buffer (0.2 M, pH 5.0). $[\boldsymbol{1}] = 12.25$ mmol L^{-1}, and $[SiVW_{11}O_{40}^{5-}] = 0.25$ mmol L^{-1}.

Table 1. The observed rate constants (k_{obs}) and second-order rate constants (k) for the oxidation of ***1*** by $SiVW_{11}O_{40}^{5-}$ in sodium acetate buffer (0.2 M, pH 5.0). [***1***] = 12.25 mmol L^{-1}, [$SiVW_{11}O_{40}^{5-}$] = 0.25 mmol L^{-1}

		Pseudo-first order late raw	
Temp.°C	Initial late raw k $(M^{-1}s^{-1})^a$	k_{obs} $(s^{-1})^b \times 10^{-2}$	k $(M^{-1}s^{-1})^c$
4	2.48 ± 0.42	5.84 ± 0.51	2.38 ± 0.21
10	3.10 ± 0.35	7.46 ± 0.14	3.04 ± 0.06
15	3.65 ± 0.09	9.15 ± 0.11	3.74 ± 0.04
20	4.76 ± 0.19	11.76 ± 0.10	4.80 ± 0.04
25	6.68 ± 0.47	15.64 ± 0.11	6.38 ± 0.04

[a]Second-order rate constants calculated from Figure A4 a in Appendix.
[b]Pseudo-first order rate constants calculated from Figure A4 b in Appendix.
[c]Second-order rate constants calculated by Eq. 6 using k_{obs}^{b}.

to POM (Scheme 1). Likewise, k_2/k_1 is $\approx 10^6$, consistent with the $k_{phenolate}/k_{phenol}$ ratio reported for the bromination of phenols and phenolate ions.[30]

It should be noted that the pK_a values used in the determination of k_2 are for room temperature conditions, therefore some error may be associated with these values. However, as k_2 is $\approx 10^6$ times larger than k_1, any error associated with the calculation of k_2 would not substantially affect the value, and would not be of the same order of magnitude or less than k_1. Finally, although these data indicate the reaction mechanism involves a rate-determining electron transfer from neutral phenol to POM, these results do not differentiate between hydrogen atom transfer and proton-coupled electron transfer mechanisms.

Activation Parameters

The effect of temperature on k_{obs} was studied from 4–90°C at pH 5.0 (acetate buffer, 0.2 M) for a series of substituted phenols. The concentrations of the

Table 2. Calculated rate constants k_1 and k_2 for the oxidation of ***1***, ***2***, ***5***, and ***8*** by $SiVW_{11}O_{40}^{5-}$ in sodium acetate buffer (0.2 M, pH 3.9–6.0). [phenols] = 12.25 mmol L^{-1}, [$SiVW_{11}O_{40}^{5-}$] = 0.25 mmol L^{-1}

Compound†	k_1 $M^{-1}s^{-1}$	$k_2{}^a$ $M^{-1}s^{-1}$	Temp.°C
1	1.59	1.21×10^6	20
2	8.61×10^{-4}	5.88×10^4	35
5	7.85×10^{-4}	5.30×10^3	45
8	0.79×10^{-4}	1.42×10^1	80

†***1*** (p-methoxylphenol), ***2*** (p-methylphenol), ***5*** (phenol), ***8*** (m-chlorophenol).
[a]Estimated using [K_a] at 25°C.

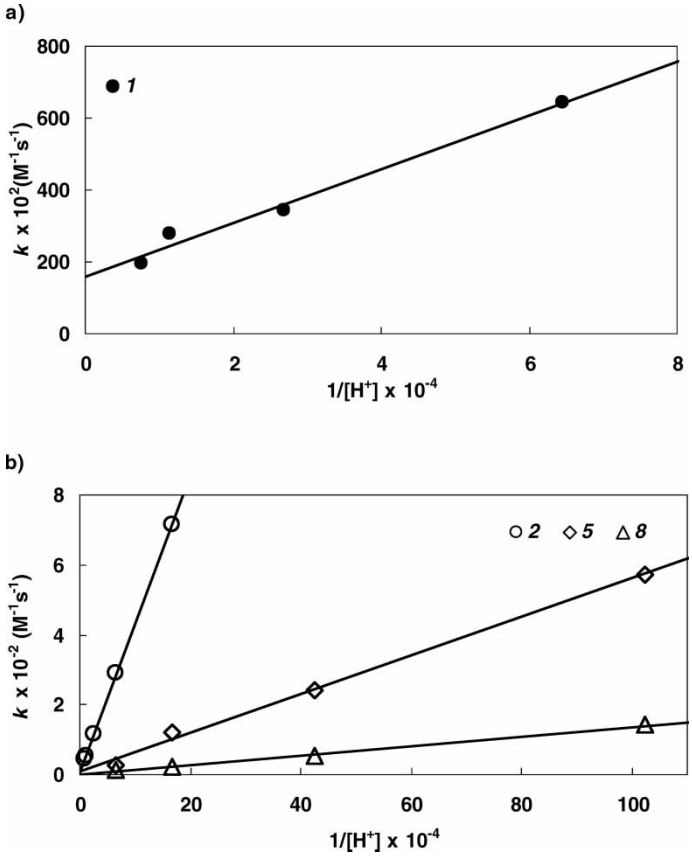

Figure 3. Effect of acidity ($1/[H^+]$) on the second order rate constant (k) for the POM ($SiVW_{11}O_{40}^{5-}$) oxidation of a) ***1***, and b) ***2***, ***5***, ***8*** at 20°C, 35°C, 45°C, and 80°C, respectively in sodium acetate buffer (0.2 M, pH 3.9–6.0). [phenols] = 12.25 mmol L^{-1}, $[SiVW_{11}O_{40}^{5-}] = 0.25$ mmol L^{-1}.

phenols and POM were 12.25 mmol L^{-1} and 0.25 mmol L^{-1}, respectively. Activation energies (E_a) were calculated from the slope of $\ln(k_{obs})$ versus $1/T$ plots according to Arrhenius Eq. (9) (Figure 4), and the activation enthalpy ($\Delta H^{\ddagger}$) and entropy ($\Delta S^{\ddagger}$) were calculated from the slope and y-intercept of $\ln(k_{obs}/T)$ versus $1/T$, respectively (according to the Erying Eq. (10) (see Appendix).[28]

$$k_r = A\, e^{-E_a/RT} \tag{9}$$

$$k_r = \frac{\kappa kT}{h}(e^{-\Delta H^{\ddagger}/RT})(e^{\Delta S^{\ddagger}/R}) \tag{10}$$

Here, k_r is the rate constant, A is the pre-exponential factor or frequency factor, E_a is the activation energy, R is the gas constant, T is absolute

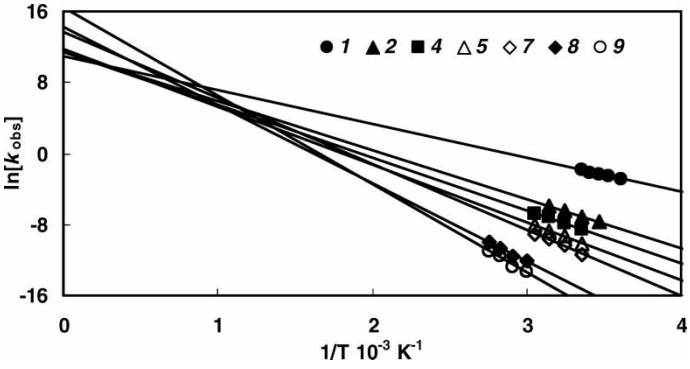

Figure 4. Isokinetic relationship (*Arrhenius* plots) of various substituted phenols.

temperature, κ is the transmission coefficient, which is usually taken to be 1, k is the Boltzmann constant, and h is the Planck constant.

From Figure 4 an isokinetic relationship (IKR) can be seen for this series of reactions. This common point or small area of intersection in the *Arrhenius* lines ($\ln(k_{obs})$ versus $1/T$) indicates that the same reaction mechanism is present in this series of compounds.[31] This is further confirmed by the linear relationship or compensation effect observed between the activation enthalpy ($\Delta H^{\ddagger}$) and entropy ($\Delta S^{\ddagger}$) (Figure 5);[32] changing the phenol substituent increases $\Delta H^{\ddagger}$ while decreasing the degree of order in the transition state ($\Delta S^{\ddagger}$). However, in both cases ***1*** does not seem to agree with the rest of the data. This may imply that the POM reaction mechanism with ***1*** is different than that of the other series of phenols, but is more likely the result of experimental error, as this compound was extremely reactive, completely consuming the POM within seconds of addition to the system.

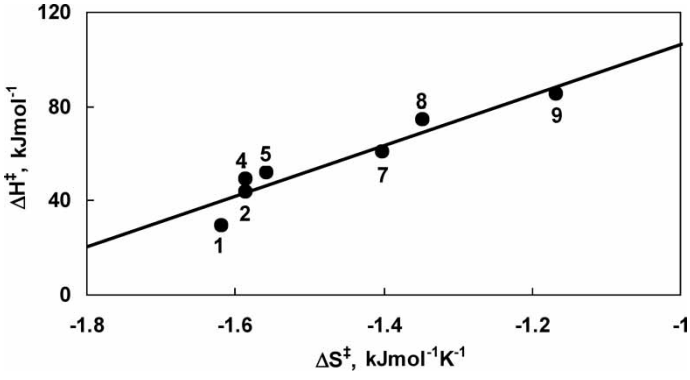

Figure 5. Activation enthalpy versus entropy for the oxidation of phenols with $SiVW_{11}O_{40}^{5-}$ in sodium acetate buffer (0.2 M, pH 5.0) at 25°C.

POM Oxidation of Substituted Phenols

One of the most widely employed relationships between substituents and reaction mechanisms/rates is the *Hammett* equation:[33,34]

$$\log(k_X/k_H) = \sigma\rho \tag{11}$$

where k_X and k_H are the rate constants for substituted and unsubstituted substrate, respectively, ρ is the reaction constant and σ is the substituent constant. The *Hammett* relationships were made by plotting log (k_X/k_H) versus σ.

For compounds ***8*** and ***9***, wherein high reaction temperatures were required to obtain satisfactory reactions, room temperature rate constants were determined from extrapolation of results obtained from a plot of $\ln(k_{obs})$ versus $1/T$ (Figure 4). The reaction rates were very sensitive to the nature of the substituent group; electron-donating groups accelerated the reaction, whereas electron-withdrawing groups decreased the reaction rate. The observed order in rate constants was ***1*** > ***2*** > ***4*** > ***3*** > ***5*** > ***6*** > ***7*** > ***8*** > ***9*** (see Appendix).

To quantify the substituent effects, the corresponding reaction constants (ρ) were determined from a plot of log (k_X/k_H) against the corresponding *Hammett* σ and σ^+ constants (Figure 6); $\rho = -6.00$ ($r^2 = 0.88$) using σ values, and -4.70 ($r^2 = 0.98$) for σ^+ values. The negative reaction constants imply that the reaction rate is favored as a result of an increase in electron density at the reaction site,[34,35] that is, electron donating substituents enhance the reaction

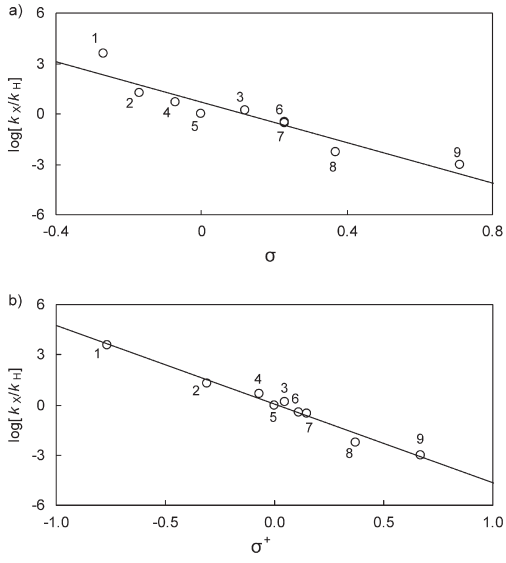

Figure 6. *Hammett* plots for the oxidation of substituted phenols with $SiVW_{11}O_{40}^{5-}$ in sodium acetate buffer (0.2 M, pH 5.0) at room temperature. The rate constants and substituent constants (σ and σ^+) are those listed in Table A3.

rate. This is consistent with an electron-transfer reaction mechanism.[27] The better correlation between rate data and σ^+ ($r^2 = 0.98$) values as compared to σ ($r^2 = 0.88$) support an electronic deficient intermediate in the transition state and a reaction mechanism leading to the formation of an electron-deficient phenoxy radical (Scheme 1). The strong correlation with σ^+ is further an indication that the reaction mechanism of all phenols oxidized by POM is essentially the same.

Product Analysis

Product analysis revealed both phenol oxidation and oxidative coupling products. In the reaction of POM with ***1*** p-benzoquinone (***10*** $\sim$ 3%), 5,5′-2-(2-hydroxy-5-methoxy-phenyl)-[1,4]benzoquinone (***11*** $\sim$ 27%), and dimethoxy-biphenyl-2,2′-diol (***12*** $\sim$ 0.7 %) were detected. Scheme 2 illustrates a possible reaction pathway leading to the observed reaction products.

The first step in the reaction of ***1*** with POM is oxidation of the phenolic substrate.[2,4,5,15] This likely involves either hydrogen atom transfer or proton-coupled electron transfer mechanisms. The resonance stabilized phenoxy radical intermediate then undergoes (i) reaction with a second POM and further oxidation to the corresponding cation and subsequent benzoquinone formation (***10***), or (ii) radical coupling with a second oxidized phenol and dimer formation (***12***). The resulting dimeric compound is then rapidly oxidized,[36] and undergoes the same oxidative reaction steps as the initial phenol, leading to oxidized biphenols (***11***) and other coupling products. In reactions run under the

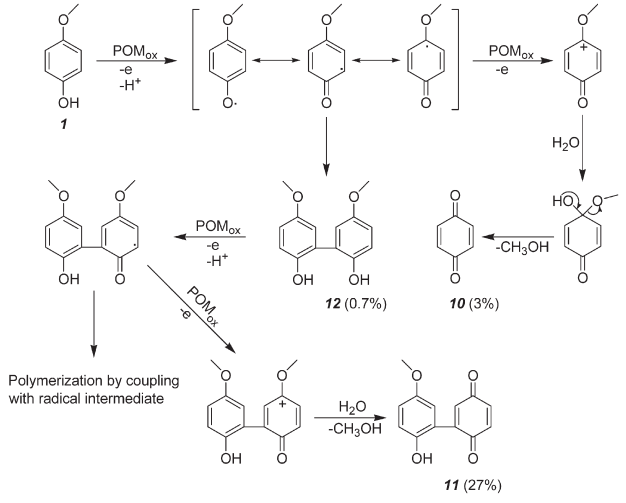

Scheme 2. Possible mechanism for the POM ($SiVW_{11}O_{40}^{5-}$) oxidation of ***1*** under anaerobic conditions.

conditions used for kinetic analysis (1:49, POM:phenol) only oxidized phenolic products were detected. However, when product analyses were performed on reactions run in an excess of POM relative to phenol (4:1, POM:phenol), the primary products detected were oxidative coupling products, which precipitated during the reaction. In fact, the yield of precipitated material was approximately 40, 50, and 70 wt% of the reaction products detected from ***1***, ***4***, and ***5***, respectively.

GPC analysis (Figure 7) of the precipitated solids confirmed they were oligomeric materials; relative average molecular masses (M_w) were 428, 741, and 549 daltons for ***1***, ***4***, and ***5***, respectively. MALDI-TOF spectra (Figure 8) further confirmed the precipitated products to be phenolic oligomers. Positive-ion linear mode MALDI-TOF spectra of the solid precipitate from ***1***, ***4***, and ***5*** contained masses corresponding to oligomeric series of each phenolic unit. The mass difference between peaks in Figure 8 (numbers 122, 106, and 92) represent the molecular weight of the respective phenolic units. Thus, in the presence of excess POM, subsequent electron transfer of the initial oxidized and oxidatively coupled products occurs. Scheme 3 shows the possible structures of the oligomeric materials formed during POM reactions of ***1***, ***4***, and ***5***.

^{1}H-NMR spectra of the oligmeric products are presented in Figure 9. The NMR spectra are broad, particularly in the aromatic region (7.5–6.6 ppm), the methoxyl region (3.8–3.2 ppm) and the methyl region (2.3–1.8 ppm). The broad and multiple peaks observed in the ^{1}H-NMR spectra of the oligomeric materials are similar to results reported for the ^{1}H-NMR analysis polyphenols.[37] These results suggest the formation of oligomers consisting of a mixture of phenylene and oxyphenylene units, as shown in Scheme 3.[37–39]

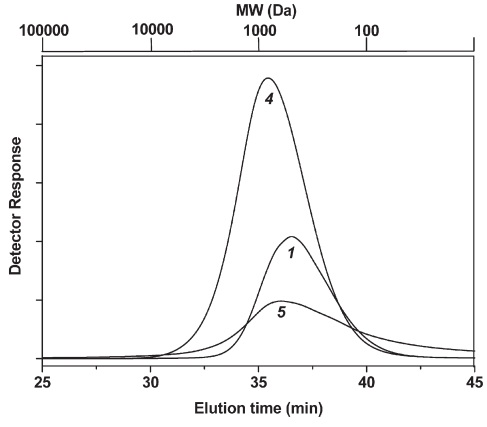

Figure 7. Gel permeation chromatography (GPC) elution curves of the precipitated materials formed during POM ($SiVW_{11}O_{40}^{5-}$) reaction with ***1*** (25°C for 1 h), ***4***, and ***5*** (60°C for 2 h and 5 h, respectively) in sodium acetate buffer (0.2 M, pH 5.0).

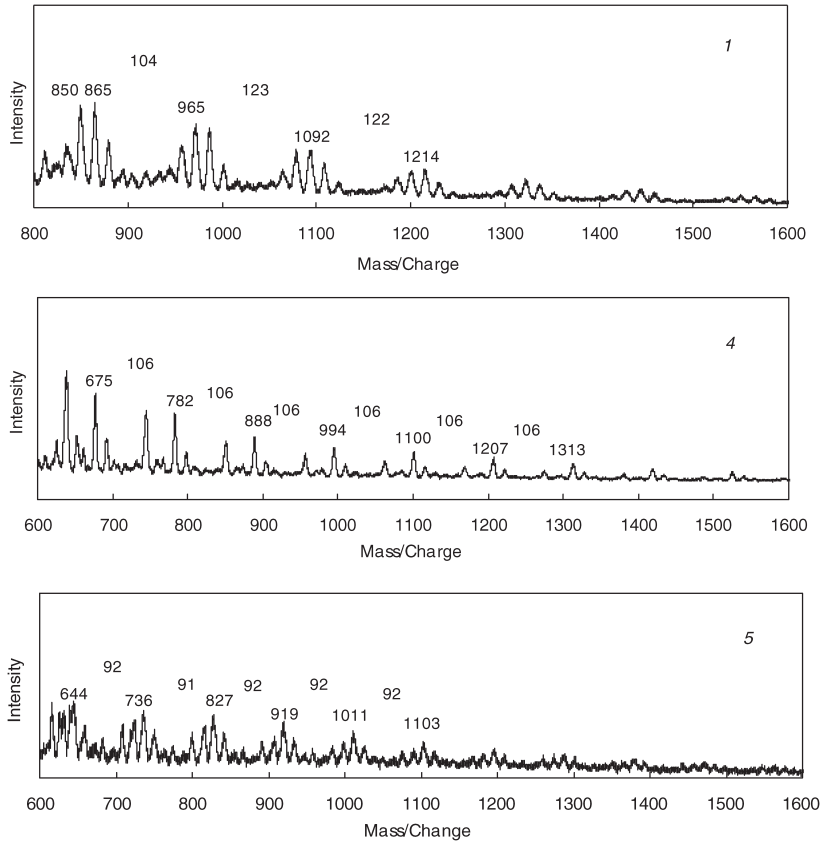

Figure 8. MALDI-TOF-MS spectra of oligomeric materials formed during the POM ($SiVW_{11}O_{40}^{5-}$) reaction with ***1*** (25°C for 1 h), ***4***, and ***5*** (60°C for 2 h and 5 h, respectively) in sodium acetate buffer (0.2 M, pH 5.0). 3,5-dimethoxy-4-hydroxycinnamic acid was the matrix for ***1*** and 2,5-dihydroxybenzoic acid was the matrix for ***4*** and ***5***.

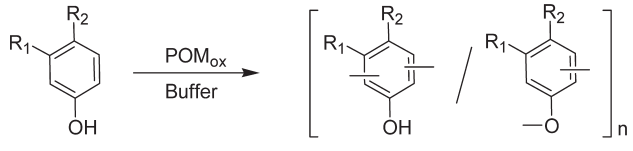

1: R_1 = H, R_2 = OCH_3
4: R_1 = CH_3, R_2 = H
5: R_1 = H, R_2 = H

Scheme 3. Possible structures of oligomeric materials formed from the reaction of POM ($SiVW_{11}O_{40}^{5-}$) with ***1*** (25°C for 1 h), ***4***, and ***5*** (60°C for 2 h and 5 h, respectively) in sodium acetate buffer (0.2 M, pH 5.0).

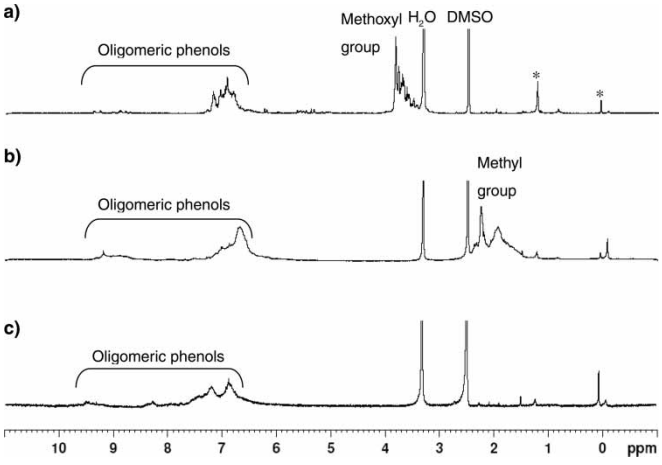

Figure 9. ^{1}H NMR spectra of the oligomers formed during the reaction of POM ($SiVW_{11}O_{40}^{5-}$) in sodium acetate buffer (0.2 M, pH 5.0) with a) ***1*** at 25°C for 1 h, b) ***4*** at 60°C for 2 h, and c) ***5*** at 60°C for 5 h. *Unknown signals or impurities.

CONCLUSIONS

The reaction kinetics and mechanism of POM oxidation of a series of substituted phenols were examined under anaerobic conditions. Using an initial rates method and pseudo-first order kinetics the rate determining step was found to be a second-order reaction in this series of phenols, first-order in substrate and oxidant. Both the *Hammett* equation and activation kinetic data indicate the same reaction mechanism exists in this series of phenols, the rate of which is highly dependent on the nature of the substituent group: electron donating groups (EDG) accelerated reaction rates whereas electron withdrawing groups (EWG) retarded reaction rates. The rate-determining step appears to involve an electron-transfer from a neutral substrate by POM. Product analyses revealed the oxidized resonance stabilized phenoxy radical intermediate then undergoes a second oxidation step to the corresponding cation and ultimately benzoquinone formation, or radical coupling with a second oxidized phenol and dimer formation. In the presence of excess POM, the resulting dimers can then undergo further reaction with POM, leading to oligomer formation.

REFERENCES

1. Cavani, F. Heteropolycompound-based catalysts: A blend of acid and oxidizing properties. Catalysis Today **1998**, *41* (1–3), 73–86.
2. Lissel, M.; Dewal, H.J.I.; Neumann, R. Oxidation of activated phenols by dioxygen catalyzed by the $H_5[PV_2Mo_{10}O_{40}]$ heteropolyanion. Tetra. Lett. **1992**, *33* (13), 1795–1798.

3. Pope, M.T. *Heteropoly and Isopolyoxometalates*; Springer-Verlag: Berlin, Heidelberg, New York, Tokyo, 1983.
4. Pope, M.T.; Muller, A. Polyoxometalate chemistry—An old field with new dimensions in several disciplines. Angew. Chem. Int. Edit. **1991**, *30* (1), 34–48.
5. Weinstock, I.A. Homogeneous-phase electron-transfer reactions of polyoxometalates. Chem. Rev. **1998**, *98* (1), 389–389.
6. Muller, A.; Peters, F.; Pope, M.T.; Gatteschi, D. Polyoxometalates: very large clusters—nanoscale magnets. Chem. Rev. **1998**, *98* (1), 239–271.
7. Grigoriev, V.A.; Cheng, D.; Hill, C.L.; Weinstock, I.A. Role of alkali metal cation size in the energy and rate of electron transfer to solvent-separated 1:1 [(M^+)(acceptor)] ($M^+ = Li^+$, Na^+, K^+) ion pairs. J. Am. Chem. Soc. **2001**, *123* (22), 5292–5307.
8. Kozhevnikov, I.V. Catalysis by polyoxometalates. In *Catalysts for Fine Chemical Synthesis Vol. 2*; Kozhevnikov, I.V., Ed.; Wiley-Interscience: New York, 2002, 10–42.
9. Katsoulis, D.E. A survey of applications of polyoxometalates. Chem. Rev. **1998**, *98* (1), 359–387.
10. Weinstock, I.A.; Atalla, R.H.; Reiner, R.S.; Moen, M.A.; Hammel, K.E.; Houtman, C.J.; Hill, C.L. A new environmentally benign technology and approach to bleaching kraft pulp. Polyoxometalates for selective delignification and waste mineralization. New J. Chem. **1996**, *20* (2), 269–275.
11. Weinstock, I.A.; Atalla, R.H.; Reiner, R.S.; Moen, M.A.; Hammel, K.E.; Houtman, C.J.; Hill, C.L.; Harrup, M.K. A new environmentally benign technology for transforming wood pulp into paper—Engineering polyoxometalates as catalysts for multiple processes. J. Mol. Catal. a—Chemical **1997**, *116* (1–2), 59–84.
12. Evtuguin, D.V.; Neto, C.P.; Rocha, J.; De Jesus, J.D.P. Oxidative delignification in the presence of molybdovanadophosphate heteropolyanions: mechanism and kinetic studies. Appl. Catal. A—Gen. **1998**, *167* (1), 123–139.
13. Lissel, M.; Dewal, H.J.I.; Neumann, R. Oxidation of activated phenols by dioxygen catalyzed by the $H_5[PV_2Mo_{10}O_{40}]$ heteropolyanion. Tetra. Lett. **1992**, *33* (13), 1795–1798.
14. Kholdeeva, O.A.; Golovin, A.V.; Maksimovskaya, R.I.; Kozhevnikov, I.V. Oxidation of 2,3,6-trimethylphenol in the presence of molybdovanadophosphoric heteropoly acids. J. Mol. Catal. **1992**, *75* (3), 235–244.
15. Weinstock, I.A.; Hammel, K.E.; Moen, M.A.; Landucci, L.L.; Ralph, S.; Sullivan, C.E.; Reiner, R.S. Selective transition-metal catalysis of oxygen delignification using water-soluble salts of polyoxometalate (POM) anions. Part II. Reactions of alpha- $SiVW_{11}O_{40}^{5-}$ with phenolic lignin-model compounds. Holzforschung **1998**, *52* (3), 311–318.
16. Evtuguin, D.V.; Neto, C.P.; De Jesus, J.D.P. Bleaching of kraft pulp by oxygen in the presence of polyoxometalates. J. Pulp Paper Sci. **1998**, *24* (4), 133–140.
17. Evtuguin, D.V.; Neto, C.P.; Carapuca, H.; Soares, J. Lignin degradation in oxygen delignification catalyzed by $[PMo_7V_5O_{40}]^{8-}$ polyanion. Part II. Study on lignin monomeric model compounds. Holzforschung **2000**, *54* (5), 511–518.
18. Evtuguin, D.V.; Neto, C.P. New polyoxometalate promoted method of oxygen delignification. Holzforschung **1997**, *51* (4), 338–342.
19. Adler, E. Lignin chemistry—past, present and future. Wood Sci. Technol. **1977**, *11* (3), 169–218.
20. Freudenberg, H.; Neish, A.C. The constitution and biosynthesis of lignin. In *Molecular Biology, Biochemistry, and Biophysics*; Kleinszeller, A., Springer, G.F. and Wittmann, H.G. Eds.; Springer-Verlag: Berlin-Heidelberg, 1968; Vol. 2, 47–122.

21. Sakakibara, A. A structural model of softwood lignin. Wood Sci. Technol. **1980**, *14* (2), 89–100.
22. Nimz, H. Beech lignin—proposal of a constitutional scheme. Angew. Chem. Int. Edit. **1974**, *13* (5), 313–321.
23. Wajon, J.E.; Rosenblatt, D.H.; Burrows, E.P. Oxidation of phenol and hydroquinone by chlorine dioxide. Environ. Sci. Technol. **1982**, *16* (7), 396–402.
24. Tee, O.S.; Paventi, M.; Bennett, J.M. Kinetics and mechanism of the bromination of phenols and phenoxide ions in aqueous-solution—diffusion-controlled rates. J. Am. Chem. Soc. **1989**, *111* (6), 2233–2240.
25. Rayne, S.; Sasaki, R.; Wan, P. Photochemical rearrangement of dibenzo-1,4-dioxins proceeds through reactive spirocyclohexadienone and biphenylquinone intermediates. Photoch. Photobio. Sci. **2005**, *4* (11), 876–886.
26. Ochiai, M.; Fukui, K.; Iwatsuki, S.; Ishihara, K.; Matsumoto, K. Synthesis of arylplatinum dinuclear complexes via ortho C-H bond activation of phenol and transmetalation of arylboronic acid. Organometallics **2005**, *24* (23), 5528–5536.
27. Yiu, D.T.Y.; Lee, M.F.W.; Lam, W.W.Y.; Lau, T.C. Kinetics and mechanisms of the oxidation of phenols by a trans-dioxoruthenium(VI) complex. Inorg. Chem. **2003**, *42* (4), 1225–1232.
28. Carey, F.A.; Sundberg, R.J. Structure and mechanism. In *Advanced Organic Chemistry Part A*; Carey, F.A. and Sundberg, R.J., Eds.; Kluwer Academic and Plenum Publishers: New York, Boston, Dordrecht, London and Moscow, 2000, 204–215.
29. Gross, K.C.; Seybold, P.G. Substituent effects on the physical properties and pK_a of phenol. Int. J. Quantum Chem. **2001**, *85* (4–5), 569–579.
30. Tee, O.S.; Paventi, M.; Bennett, J.M. Kinetics and mechanism of the bromination of phenols and phenoxide ions in aqueous-solution—diffusion-controlled rates. J. Am. Chem. Soc. **1989**, *111* (6), 2233–2240.
31. Linert, W. Mechanistic and structural investigations based on the isokinetic relationship. Chem. Soc. Rev. **1994**, *23* (6), 429–438.
32. Ganiev, I.M.; Suvorkina, E.S.; Kabal'nova, N.N. Reaction of chlorine dioxide with phenol. Russ. Chem. Bulletin **2003**, *52* (5), 1123–1128.
33. Hansch, C.; Leo, A.; Taft, R.W. A survey of Hammett substituent constants and resonance and field parameters. Chem. Rev. **1991**, *91* (2), 65–195.
34. Hammett, L.P. The effect of structure upon the reactions of organic compounds—benzene derivatives. J. Am. Chem. Soc. **1937**, *59*, 96–103.
35. Jovanovic, S.V.; Tosic, M.; Simic, M.G. Use of the Hammett correlation and σ^+ for calculation of one-electron redox potentials of antioxidants. J. Phys. Chem. **1991**, *95* (26), 10824–10827.
36. Kim, Y.S.; Chang, H.-M.; Kadla, J.F. Polyoxometalate (POM) oxidation of lignin model compounds. Holzforschung **2008**, *62* (1), 38–49.
37. Kim, Y.; Uyama, H.; Kobayashi, S. Peroxidase-catalyzed oxidative polymerization of phenol with a nonionic polymer surfactant template in water. Macromol. Biosci. **2004**, *4*, 497–502.
38. Mita, N.; Tawaki, S.; Uyama, H.; Kobayashi, S. Structural control in enzymatic oxidative polymerization of phenols with varying the solvent and substituent nature. Chem. Lett. **2002**, *3*, 402–403.
39. Mita, N.; Tavaki, S.; Kobayashi, S. Enzymatic oxidative polymerization of phenols in an aqueous solution in the presence of a catalytic amount of cyclodextrin. Macromol. Biosci. **2002**, *2* (3), 127–130.

APPENDIX

Table A1. Dimers (**14***) formed during the POM ($SiVW_{11}O_{40}^{5-}$) oxidation of **4** (m-methylphenol)

Mass spectral data
214(M^+, 86), 199(100), 181(50), 171(13), 153(14), 128(8), 115(6), 107(2), 77(3)
214(M^+, 100), 199(19), 181(12), 171(6), 153(5), 122(50), 94(16), 77(6), 66(8)
214(M^+, 100), 199(61), 181(26), 171(25), 153(11), 128(10), 115(8), 91(3), 77(3)
214(M^+, 57), 199(100), 184(8), 171(53), 143(14), 128(25), 115(11), 91(3), 77(3)
214(M^+, 100), 199(92), 181(36), 171(16), 152(12), 128(8), 115(9), 77(4)
214(M^+, 100), 199(64), 181(35), 153(12), 141(8), 128(4), 115(8), 91(2), 77(3)

Table A2. Observed kinetic constants for the oxidation of substituted phenols by $SiVW_{11}O_{40}^{5-}$ in sodium acetate buffer (0.2 M, pH 5.0)

Compound	Temp. °C	Rate constants k_{obs} (s^{-1})	$\Delta H^{\ddagger}$ $kJ \cdot mol^{-1}$	$\Delta S^{\ddagger}$ $J \cdot mol^{-1}$ K^{-1}	Ea $kJ \cdot mol^{-1}s^{-1}$
1	4	$(5.84 \pm 0.51) \times 10^{-2}$	29 ± 2	-162 ± 7	32 ± 2
	10	$(7.46 \pm 0.14) \times 10^{-2}$			
	15	$(9.15 \pm 0.11) \times 10^{-2}$			
	20	$(11.76 \pm 0.10) \times 10^{-2}$			
	25	$(15.64 \pm 0.11) \times 10^{-2}$			
2	15	$(4.00 \pm 0.26) \times 10^{-4}$	44 ± 1	-158 ± 3	46 ± 1
	25	$(7.65 \pm 0.33) \times 10^{-4}$			
	35	$(1.54 \pm 0.04) \times 10^{-3}$			
	45	$(2.61 \pm 0.06) \times 10^{-3}$			
4	25	$(1.90 \pm 0.26) \times 10^{-4}$	47 ± 3	-158 ± 9	49 ± 3
	35	$(4.08 \pm 0.88) \times 10^{-4}$			
	45	$(7.38 \pm 0.33) \times 10^{-4}$			
	55	$(1.18 \pm 0.02) \times 10^{-3}$			
5	25	$(4.17 \pm 0.06) \times 10^{-5}$	52 ± 1	-156 ± 4	54 ± 1
	35	$(9.00 \pm 0.11) \times 10^{-5}$			
	45	$(1.63 \pm 0.03) \times 10^{-4}$			
	55	$(3.13 \pm 0.04) \times 10^{-4}$			
7	25	$(1.21 \pm 0.06) \times 10^{-5}$	59 ± 1	-140 ± 4	62 ± 1
	35	$(3.33 \pm 0.11) \times 10^{-5}$			
	45	$(6.67 \pm 0.03) \times 10^{-5}$			
	55	$(1.20 \pm 0.04) \times 10^{-4}$			
8	25[a]	2.38×10^{-7}	70 ± 1	-136 ± 3	73 ± 1
	60	$(5.78 \pm 0.08) \times 10^{-6}$			
	70	$(1.01 \pm 0.03) \times 10^{-5}$			
	80	$(2.29 \pm 0.04) \times 10^{-5}$			
	90	$(5.00 \pm 0.02) \times 10^{-5}$			
9	25[a]	4.13×10^{-8}	80 ± 1	-120 ± 3	83 ± 1
	60	$(1.56 \pm 0.02) \times 10^{-6}$			
	70	$(2.56 \pm 0.04) \times 10^{-6}$			
	80	$(9.00 \pm 0.04) \times 10^{-6}$			
	90	$(1.60 \pm 0.02) \times 10^{-6}$			

[a]Extrapolated from a plot of $\ln(k_{obs})$ versus $1/T$.

Table A3. Second-order rate constants for the reaction between $SiVW_{11}O_{40}^{5-}$ and substituted phenols in sodium acetate buffer (0.2 M, pH 5.0) at 25°C

			Substituent constants[26]	
Compound†	Rate constants k_{obs} (s^{-1})	$\log[k_X/k_H]$	σ	σ^+
1	$(1.56 \pm 0.04) \times 10^{-1}$	3.57	−0.27	−0.76
2	$(7.65 \pm 0.14) \times 10^{-4}$	1.26	−0.17	−0.31
3	$(6.38 \pm 0.01) \times 10^{-5}$	0.19	0.12	0.05
4	$(1.90 \pm 0.93) \times 10^{-4}$	0.66	−0.07	−0.07
5	$(4.17 \pm 0.02) \times 10^{-5}$	0.00	0.00	0.00
6	$(1.43 \pm 0.29) \times 10^{-5}$	−0.46	0.23	0.11
7	$(1.21 \pm 0.45) \times 10^{-5}$	−0.54	0.23	0.15
8	2.38×10^{-7}[a]	−2.24	0.37	0.37
9	4.13×10^{-8}[a]	−3.00	0.71	0.67

[a]Extrapolated from a plot of $\ln(k_{obs})$ versus $1/T$ (Figure 4).

1 (*p*-methoxylphenol), ***2*** (*p*-methylphenol), ***3*** (*m*-methoxylphenol), ***4*** (*m*-methylphenol), ***5*** (phenol), ***6*** (*p*-chlorophenol), ***7*** (*p*-bromophenol), ***8*** (*m*-ch chlorophenol), and ***9*** (*m*-nitrophenol).

Table A4. Oligomerization of ***1*** (25°C for 1 h), ***4***, and ***5*** (60°C for 2 h and 5 h, respectively) using POM ($SiVW_{11}O_{40}^{5-}$) in sodium acetate buffer (0.2 M, pH 5.0)

Compounds	M_w[a]	# of units[b]
1	428	4
4	741	7
5	549	6

[a]Determined by GPC using THF as eluent with polystryrene standards.

[b]Number of units calculated from M_w divided by molecule weight of each monomer.

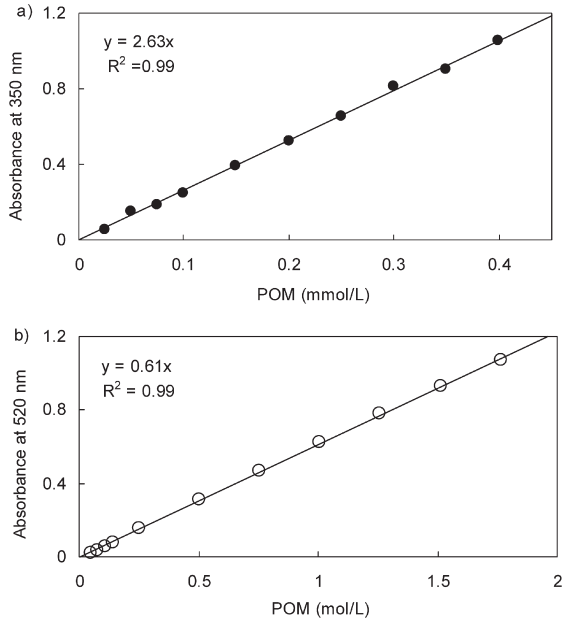

Figure A1. Relationship between concentration of POM and absorbance at a) 350 nm ($SiVW_{11}O_{40}^{5-}$) and b) 520 nm ($SiVW_{11}O_{40}^{6-}$).

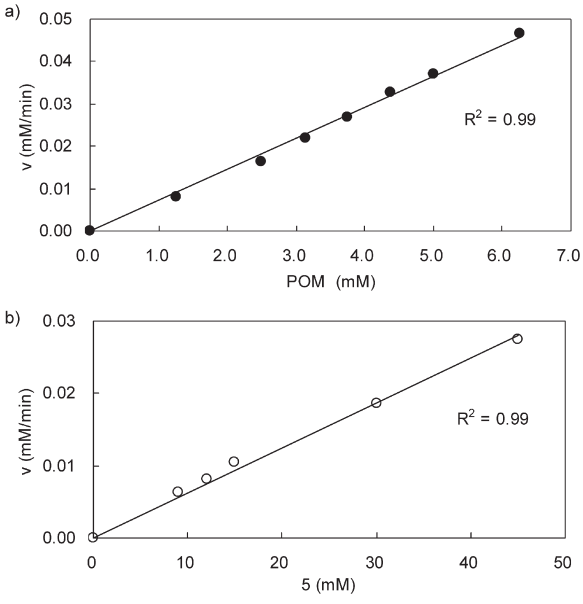

Figure A2. Plot of initial rate versus a) [POM] or b) [***5***] at 25°C in sodium acetate buffer (0.2 M, pH 5.0). ***5*** (phenol).

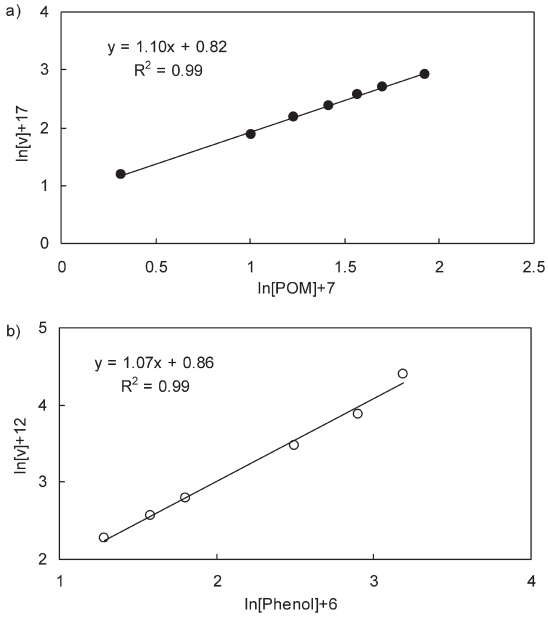

Figure A3. Plot of ln[initial rate] versus a) ln[POM] and b) ln[***5***] at 25°C in sodium acetate buffer (I = 0.2 M, pH 5.0). ***5*** (phenol).

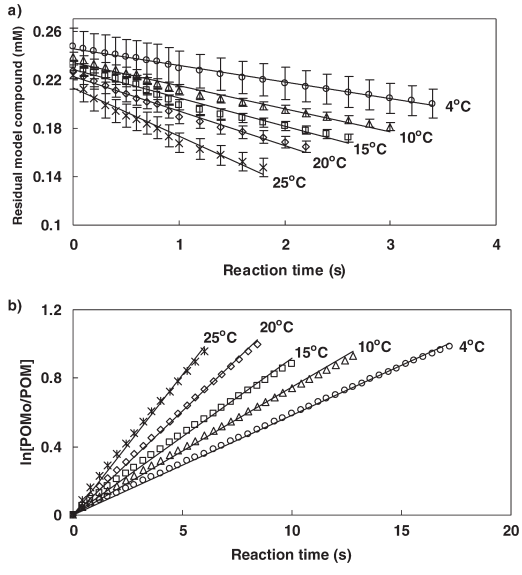

Figure A4. Kinetic analysis of $SiVW_{11}O_{40}^{5-}$ oxidation of ***1*** at different temperatures (°C) in sodium acetate buffer (0.2 M, pH 5.0): a) initial rate plot and b) pseudo-first order plot. [***1***] = 12.25 mmol L^{-1}, and $[SiVW_{11}O_{40}^{5-}]$ = 0.25 mmol L^{-1}. ***1*** (*p*-methoxylphenol).